BIOCHEMISTRY
including biophysical chemistry & molecular biology

Article

pubs.acs.org/biochemistry

Redefining the Role of the Quaternary Shift in *Bacillus stearothermophilus* Phosphofructokinase

Rockann Mosser,[†] Manchi C. M. Reddy, John B. Bruning,[‡] James C. Sacchettini, and Gregory D. Reinhart*

Department of Biochemistry and Biophysics, Texas A&M University, and Texas A&M AgriLife Research, College Station, Texas 77843-2128, United States

ABSTRACT: *Bacillus stearothermophilus* phosphofructokinase (BsPFK) is a homotetramer that is allosterically inhibited by phosphoenolpyruvate (PEP), which binds along one dimer−dimer interface. The substrate, fructose 6-phosphate (Fru-6-P), binds along the other dimer−dimer interface. Evans et al. observed that the structure with inhibitor (phosphoglycolate) bound, compared to the structure of wild-type BsPFK with substrate and activator bound, exhibits a 7° rotation about the substrate-binding interface, termed the quaternary shift [Schirmer, T., and Evans, P. R. (1990) *Nature 343*, 140−145]. We report that the variant D12A BsPFK exhibits a 100-fold increase in its binding affinity for PEP, a 50-fold decrease in its binding affinity for Fru-6-P, but an inhibitory coupling comparable to that of the wild type. Crystal structures of the apo and PEP-bound forms of D12A BsPFK have been determined (Protein Data Bank entries 4I36 and 4I7E, respectively), and both indicate a shifted structure similar to the inhibitor-bound structure of the wild type. D12 does not directly bind to either substrate or inhibitor and is located along the substrate-binding interface. A conserved hydrogen bond between D12 and T156 forms across the substrate-binding subunit−subunit interface in the substrate-bound form of BsPFK. The variant T156A BsPFK, when compared to the wild type, shows a 30-fold increase in PEP binding affinity, a 17-fold decrease in Fru-6-P binding affinity, and an estimated coupling that is also approximately equal to that of the wild type. In addition, the T156A BsPFK crystal structure bound to PEP is reported (Protein Data Bank entry 4I4I), and it exhibits a shifted structure similar to that of D12A BsPFK and the inhibitor-bound structure of the wild type. The results suggest that the main role of the quaternary shift may be to influence ligand binding and not to cause the heterotropic allosteric inhibition per se.

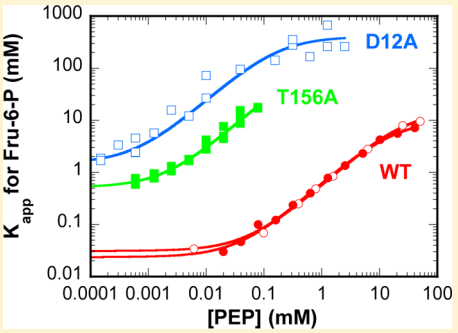

Phosphofructokinase 1 (PFK) is a highly regulated enzyme that catalyzes the first committed step of glycolysis in prokaryotes. It is one of two nonhomologous gene products that catalyze the transfer of the γ-phosphate of MgATP to fructose 6-phosphate (Fru-6-P), producing fructose-1,6-bisphosphate and MgADP. PFK from the moderate thermophile *Bacillus stearothermophilus* (Bs) is a homotetramer of 34 kDa per subunit that forms a dimer of dimers creating two unique subunit−subunit interfaces. One subunit−subunit interface contains four identical binding sites for Fru-6-P per homotetramer. The other subunit−subunit interface contains the four identical binding sites for the allosteric ligands per homotetramer. The allosteric binding sites physiologically are capable of binding either MgADP or phosphoenolpyruvate (PEP). For BsPFK, MgADP serves as a very weak activator and PEP is a very strong inhibitor at 25 °C. Both PEP and MgADP alter the affinity that BsPFK displays for Fru-6-P without changing the enzyme's maximal activity; therefore, both allosteric ligands are considered to be K-type effectors.

The regulation of PFK has been the subject of study for nearly five decades since Blangy et al. first characterized the kinetics of PFK from *Escherichia coli* and explained the behavior using a two-state model[1] in which the two states undergo a concerted transition in accordance with the model proposed by Monod, Wyman, and Changeux.[2] Schirmer and Evans compared the crystal structure of PFK bound to the inhibitor analogue phosphoglycolate (PGA) [Protein Data Bank (PDB) entry 6PFK][3] with that obtained with BsPFK bound to Fru-6-P and activator MgADP (PDB entry 4PFK)[4,5] and found a substantial conformational difference. The conformational change includes a difference in the quaternary structures of the two enzyme forms. The quaternary structure of inhibitor-bound BsPFK has undergone a 7° rotation about the substrate-binding interface, termed the quaternary shift, when compared to the substrate- and activator-bound BsPFK. The conformational change also includes the movement of residues E161 and R162 in the active site. When Fru-6-P is bound to the enzyme, the positively charged side chain of R162 interacts with the negatively charged phosphate group of Fru-6-P. In the PGA-bound structure, R162 effectively is replaced with the negatively charged side chain of E161. Given the structural differences seen between the substrate- and activator-bound and inhibitor-bound structures of BsPFK, Schirmer and Evans proposed that these two structures corresponded to the two states that Blangy et al. had invoked to explain the allosteric behavior of PFK.[3]

Received: February 27, 2013
Revised: July 15, 2013
Published: July 16, 2013

   dx.doi.org/10.1021/bi4002503 | *Biochemistry* 2013, 52, 5421−5429

Since 1990, BsPFK often has been used as a textbook example of the structural basis for allosteric regulation.[6,7]

A key distinction that should be made when assessing the allosteric action of a ligand, such as the inhibitor PEP, is between the affinity it displays for the enzyme and the effectiveness with which it inhibits once it binds. The latter attribute is quantitatively conveyed by the coupling between the inhibitor and substrate.[8] We have previously shown that the repositioning of R162 and E161 has a surprisingly small role to play in the inhibitory coupling between Fru-6-P and PEP.[9] This investigation suggests that the quaternary shift similarly does not appear to be the basis for the coupling between Fru-6-P and PEP.

A significant structural perturbation associated with the quaternary shift is the disruption of several intersubunit hydrogen bonds involving residue D12. Previous work performed by Ortigosa et al. noted the significance of D12 upon construction of certain hybrid forms of BsPFK.[10] In that study, a D12A mutation was made in concert with other mutations to allow the proper exchange of subunits when making hybrids. The characteristics of the single-site mutant were never fully investigated. We report herein the properties of D12A that include the X-ray crystal structures of D12A BsPFK with and without PEP bound (PDB entries 4I36 and 4I7E, respectively). Both structures exhibit a quaternary structure similar to that introduced by the binding of PGA to the wild-type enzyme. While the D12A mutation alters the binding of PEP and Fru-6-P, it has very little effect on the allosteric coupling.

In an effort to further understand the role of D12, a residue that is 100% conserved in more than 150 prokaryotic PFK-1 sequences, we also have examined the behavior of variants of BsPFK in which those residues with which D12 interacts across the interface have been changed to alanine. Generally, these variants also exhibit comparable or greater coupling between Fru-6-P and PEP. The structure of one of these variants, T156A, bound to PEP has also been determined (PDB entry 4I4I), and not surprisingly, it also exhibits the quaternary shift.

It is of note that both D12A and T156A for the first time allowed structures of BsPFK to be determined in which the native inhibitor, PEP, is bound.

MATERIALS AND METHODS

Materials. All chemical reagents used in buffers, protein purifications, and enzymatic assays were of analytical grade, purchased from Sigma-Aldrich (St. Louis, MO) or Fisher Scientific (Fair Lawn, NJ). Creatine kinase and the ammonium sulfate suspension of glycerol-3-phosphate dehydrogenase were purchased from Roche (Indianapolis, IN). The ammonium sulfate suspensions of aldolase and triosephosphate isomerase and the sodium salts of phosphocreatine, ATP, and PEP were purchased from Sigma-Aldrich. The coupling enzymes were extensively dialyzed against 50 mM MOPS-KOH (pH 7.0), 100 mM KCl, 5 mM $MgCl_2$, and 0.1 mM EDTA before being used. The sodium salt of Fru-6-P was purchased from Sigma-Aldrich or USB Corp. (Cleveland, OH). NADH and DTT were purchased from Research Products International (Mt. Prospect, IL), and the crystallization materials were purchased from Hampton Research (Aliso Viejo, CA). DE52 and Memetic Blue 1 resin used in protein purifications were purchased from Whatman (Maidstone, England) and Promatic BioSciences (Rockville, MD), respectively. Site-directed mutagenesis was performed using the QuikChange site-directed mutagenesis system from Stratagene (La Jolla, CA). Oligonucleotides were synthesized and purchased from Integrated DNA Technologies, Inc. (Coralville, IA). DNA-modifying enzymes and dNTPs were purchased from Stratagene (Cedar Creek, TX), New England Biolabs (Ipswich, MA), or Promega (Madison, WI). Deionized distilled water was used throughout.

Site-Directed Mutagenesis. Plasmid pBR322/BsPFK[11] contains the gene for BsPFK behind the native *B. stearothermophilus* promoter and was a generous gift from S. H. Chang (Louisiana State University, Baton Rouge, LA). Mutagenesis was performed following the QuikChange site-directed mutagenesis protocol. Two complementary oligonucleotides were used to make the mutant genes, and only the template oligo is shown below. The underlined bases designate the codon for the alanine that replaced the specific residue indicated: D12A, G TTG ACA AGC GGC GGC GCC TCG CCG GGA ATG; T156A,: C GAC AAA ATC CGC GAC GCC GCG ACG TCG; T158A, CGC GAC ACG GCG GCC TCG CAC GAG; S159A, GAC ACG GCG ACG GCC CAC GAG CGG AC; H160A, CG GCG ACG TCG GCC GAC CGG ACG TAC G. Wild-type and all mutant BsPFKs were expressed in *E. coli* RL257 cells,[12] which is a strain of *E. coli* lacking both the PFK-1 and PFK-2 genes.

Protein Purification for Wild-Type, T158A, S159A, and H160A BsPFK. The purification of both wild-type and variant BsPFKs was performed as described previously, with a few modifications.[13] RL257 cells containing the appropriate plasmid were grown at 37 °C for 16−18 h in LB (Lysogeny Broth) ampicillin (10 g/L Tryptone, 5 g/L yeast extract, 10 g/L sodium chloride, and 100 μg/mL ampicillin). Cells were pelleted and frozen for at least 12 h. The cells were resuspended in purification buffer [10 mM Tris-HCl and 1 mM EDTA (pH 8.0)] and sonicated at 0 °C in 15 s pulses for 8 min with a Fisher 550 Sonic Dismembrator. The crude lysate was centrifuged using a Beckman model J2-21 centrifuge equipped with a JA20 rotor at 22500*g* for 1 h at 4 °C. The clear supernatant was heated at 70 °C for 15 min, cooled on ice for 15 min, and centrifuged as before. The diluted supernatant for the wild-type protein was loaded onto a Mimetic Blue 1 column. The column was equilibrated with purification buffer before the supernatant containing the protein of interest was loaded. The column was washed with at least 5 bed volumes of purification buffer, and the enzyme was eluted with a 0 to 1 M NaCl gradient. Enzyme-containing fractions were pooled and dialyzed into 20 mM Tris-HCl (pH 8.5) and loaded onto a Pharmacia Mono-Q anion exchange column. The enzyme was eluted with a 0 to 1 M NaCl gradient, and PFK-containing fractions were combined, concentrated, and then dialyzed into EPPS buffer [50 mM EPPS, 10 mM $MgCl_2$, 100 mM KCl, and 0.1 mM EDTA (pH 8.0)]. The concentrated enzyme was stored in EPPS buffer at 4 °C. The final enzyme was determined to be pure by SDS−PAGE, and the concentration was ascertained using the absorbance at 280 nm (ε = 18910 M^{-1} cm^{-1}).[14]

Protein Purification for D12A and T156A BsPFK. Protein purification for D12A BsPFK and T156A BsPFK was conducted as described above, with the following exceptions. T156A BsPFK lost a significant amount of activity during the heating step unless 1 mM Fru-6-P was added to the supernatant before it was heated. Fru-6-P was not added to any other buffer for the duration of the purification for T156A BsPFK. D12A BsPFK and T156A BsPFK did not respond to the Mimetic Blue 1 resin the same as the wild type, so that the supernatant was

loaded onto a DE52 column. The DE52 column was prepared and treated the same as the Mimetic Blue 1 column.

Crystallization and Data Collection. The apo and PEP-bound D12A BsPFKs and T156A BsPFK were crystallized using the hanging drop vapor diffusion method at 16 °C. Apo D12A BsPFK was obtained through extensive dialysis of the mutant enzyme in EPPS buffer containing 50 mM EPPS, 10 mM $MgCl_2$, 100 mM KCl, 0.1 mM EDTA, and 10 mM Fru-6-P (pH 8.0) followed by extensive dialysis in Fru-6-P free EPPS buffer. The crystallization condition for the apo D12A BsPFK structure was a 4 μL drop consisting of 2 μL of solvent [0.2 M magnesium chloride hexahydrate, 0.1 M Tris hydrochloride (pH 8.5), and 30% (w/v) polyethylene glycol 4000] and 2 μL of protein (the stock concentration of apo D12A BsPFK was 35 mg/mL stored in EPPS buffer). PEP-bound D12A BsPFK was obtained through purification of the enzyme as directed above. The PEP bound to the enzyme is endogenous *E. coli* PEP. The crystallization condition for the PEP-bound D12A structure was a 6 μL drop consisting of 2 μL of solvent [0.1 M sodium citrate tribasic dehydrate (pH 5.6), 20% (v/v) 2-propanol, and 20% (w/v) polyethylene glycol 4000] and 4 μL of protein (the stock concentration of D12A BsPFK was 34 mg/mL stored in EPPS buffer). The crystallization condition for the T156A BsPFK structure was 2 μL of solvent [0.1 M HEPES sodium (pH 7.5) and 1.4 M sodium citrate tribasic dehydrate] and either 3 or 4 μL of protein (the stock concentration of T156A BsPFK was 13 mg/mL). The T156A BsPFK crystal structure is bound to four PEP molecules, just like PEP-bound D12A BsPFK. Just as D12A BsPFK is bound to the endogenous *E. coli* PEP, so is T156A BsPFK. Numerous attempts were made to crystallize T156A BsPFK without the inhibitor bound; however, none were successful. In addition, attempts were made to crystallize variants T158A, S159A, and H160A BsPFK. All proteins yielded crystals, but the quality of the crystals was insufficient and did not produce high-quality data.

Within 2−3 days, crystals formed for both species (D12A and T156A BsPFK) of the enzyme. Variant BsPFK crystals were briefly soaked in cryogenic mother liquor containing 30% ethylene glycol and then flash-frozen in a liquid N_2 stream at 100 K. Diffraction data for the apo and PEP-bound D12A BsPFK crystals were collected on Advanced Photon Source (APS) beamline 23-ID (insertion device) using a MAR 300 CCD detector (MarMosaic from Marresearch, charged coupled device) (Rayonix LLC, Evanston, IL). The high-resolution data of T156A BsPFK were collected on beamline 19-ID on an Area Detector Systems Corp. model Q315 area detector at the Advanced Photon Source (Argonne National Laboratory, Argonne, IL). The HKL2000 program package (HKL Research, Inc., Charlottesville, VA)[15] was used for integration and scaling of the PEP-bound D12A crystals, while d*TREK (Rigaku Americas, The Woodlands, TX) was used for integration and scaling of the apo D12A and T156A crystals.[15,16] Data collection details are summarized in Table 1.

Structure Determination and Refinement. Molecular replacement program PHASER (University of Cambridge, Cambridge, U.K.)[17] was used to determine the structure of the apo and PEP-bound BsPFKs using the phosphate-bound crystal structure of BsPFK (PDB entry 3PFK)[5] with waters and ions removed as the search model. Rigid body refinement followed by simulated annealing refinement at 5000 K was conducted using Phenix (Python-based Hierarchical Environment for Integrated Xtallography)[18] for the apo structure, while CCP4 Refmac (York Structural Biology Laboratory, University of York, Heslington, U.K.) with TLS refinement (translation, libration, and screw-rotation) (Science and Technology Facilities Council, Daresbury, U.K.) was used for the refinement of the PEP-bound protein.[19,20] Subsequently, refinement was conducted in alternating cycles of manual model building in COOT (Crystallographic Object-Orientated Toolkit)[21] followed by refinement until the *R* factors converged. The stereochemistries of the final models of the BsPFK enzymes were verified with MolProbity (Duke University, Durham, NC).[22]

Table 1. Data Collection and Refinement Statistics for D12A and T156A BsPFK Structures[a]

	apo D12A	D12A−PEP	T156A−PEP
Data Collection			
unit cell (Å)	a = 96.05	a = 96.65	a = 96.405
	b = 112.66	b = 112.97	b = 111.575
	c = 129.73	c = 131.04	c = 129.448
space group	$P2_12_12_1$	$P2_12_12_1$	$P2_12_12_1$
no. of molecules per asymmetric unit (Z)	four monomers	four monomers	four monomers
resolution (Å)	40−2.3	65−2.0	45−2.5
completeness (%)	100.0 (100.0)	97.0 (78.2)	100.0 (100.0)
$I/\sigma I$	12.2 (3.1)	13.3 (2.7)	36.49 (5.68)
R_{merge}[b]	7.3 (44.0)	5.3 (38.9)	10.6 (46)
Refinement			
resolution (Å)	40−2.3	50−2.00	45−2.5
no. of reflections (working/free)	63108 (3204)	89745 (4715)	
R (%)[c]	20.07	18.86	16.6
R_{free} (%)[d]	25.39	23.48	23.78
no. of protein atoms/ number of waters	9517/329	9574/626	9429/312
average B factor (Å^2)	48.41	28.96	50.5
average B factor for water molecules (Å^2)	44.21	43.53	53.1
root mean square deviation			
bond lengths (Å)	0.004	0.012	0.005
bond angles (deg)	0.517	1.355	0.637
Ramachandran statistics (%)			
most favored	97.3	97.2	97.79
allowed	2.5	2.8	0.08

[a]Values in parentheses are for high-resolution shells. [b]$R_{sym} = \sum_h\sum_i|I_{hi} - \langle I_h\rangle|/\sum_h\sum_i I_{hi}$, where I_{hi} is the ith observation of reflection h and $\langle I_h\rangle$ is the mean intensity of reflection h. [c]$R_{cryst} = \sum||F_o| - |F_c||/|F_o|$. [d]$R_{free}$ was calculated with a fraction (5%) of randomly selected reflections excluded from refinement.

Kinetic Assays. Activity measurements for PFK were taken in a 0.6 mL reaction volume of EPPS buffer containing 50 mM EPPS, 10 mM $MgCl_2$, 100 mM KCl, 0.1 mM EDTA, 2 mM DTT, 0.2 mM NADH, 3 mM ATP, 250 μg of aldolase, 50 μg of glycerol-3-phosphate dehydrogenase, 5 μg of triosephosphate isomerase, 40 μg/mL creatine kinase, and 4 mM phosphocreatine at pH 8.0 and 25 °C. Fru-6-P and PEP were added at varied concentrations as indicated. Assays were started by the addition of 6 μL of appropriately diluted PFK, and the reaction was monitored as the absorbance at 340 nm decreased over time. Dilution of T156A BsPFK in EPPS buffer resulted in a significant loss of activity; therefore, all dilutions of T156A BsPFK were done in EPPS buffer containing 1 mM Fru-6-P. The addition of Fru-6-P resulted in T156A BsPFK remaining

dx.doi.org/10.1021/bi4002503 | *Biochemistry* 2013, 52, 5421−5429

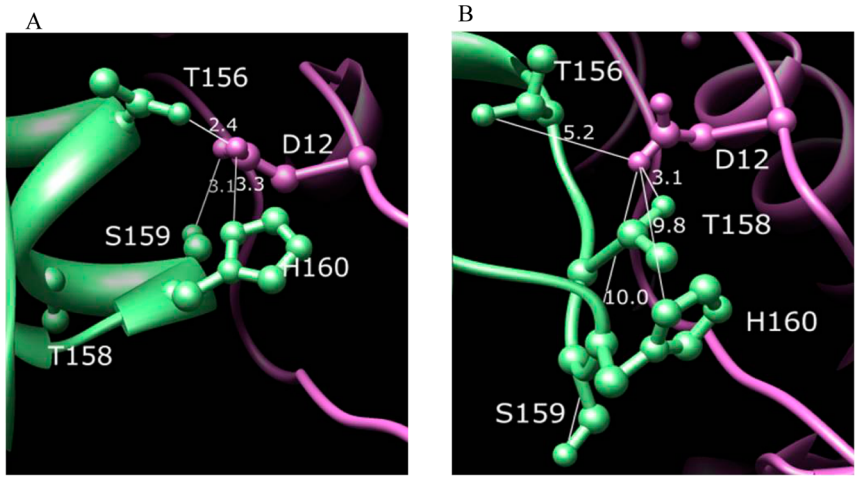

Figure 1. Crystal structure of the D12 region in wild-type BsPFK. (A) Structure of wild-type BsPFK bound to Fru-6-P and MgADP. Structural data obtained from PDB entry 4PFK. (B) Structure of wild-type BsPFK bound to PGA. Structural data obtained from PDB entry 6PFK. Distances are in angstroms.

stable throughout the duration of the assays. The rate of the reaction was measured on Beckman Series 600 spectrophotometers. One unit of PFK activity is described as the amount of enzyme needed to produce 1 μmol of F16BP/min.

Data Analysis. Data were fit to the following equations using the least-squares fitting analysis of Kaleidagraph (Synergy). Initial velocity activities, which were measured in the kinetic assays in which the Fru-6-P concentration was saturable, were fit to the Hill equation:[23]

$$\frac{v}{E_T} = \frac{k_{cat}[A]^{n_H}}{K_{1/2}{}^{n_H} + [A]^{n_H}} \quad (1)$$

where v is the initial rate, E_T is the total enzyme active site concentration, [A] is the concentration of the substrate Fru-6-P, k_{cat} is the turnover number, $K_{1/2}$ is the concentration of Fru-6-P that gives one-half the maximal specific activity, and n_H is the Hill coefficient. In the D12A BsPFK kinetic assays, $K_{1/2}$ cannot be determined because its value is too large; therefore, the data were fit to the following equation:

$$\frac{v}{E_T} = \frac{k_{cat}}{K_{1/2}}[A] \quad (2)$$

Analysis of the Allosteric Response. The heterotropic allosteric responses of BsPFK to PEP were quantified with reference to the single-substrate, single-modifier mechanism as described previously.[8,24,25] For an enzyme like BsPFK, which exhibits heterotropic allosteric effects exclusively as a perturbation of the apparent affinity for the substrate, Fru-6-P, the allosteric response can be quantified by two parameters: the dissociation constant for PEP in the absence of Fru-6-P, K^0_{iy}, and the coupling parameter, Q_{ay}. Q_{ay} is defined as follows:

$$Q_{ay} = \frac{K^0_{ia}}{K^\infty_{ia}} = \frac{K^0_{iy}}{K^\infty_{iy}} \quad (3)$$

where K^0_{ia} equals the dissociation constant for Fru-6-P in the absence of PEP, K^∞_{ia} equals the dissociation constant for Fru-6-P in the saturating presence of PEP, K^∞_{iy} equals the dissociation constant for PEP in the saturating presence of Fru-6-P, and the second equality is required by the principal of thermodynamic linkage. Equation 3 indicates that Q_{ay} quantitatively reveals both the nature of the allosteric effect (values of <1 imply inhibition and values of >1 activation) and the magnitude of the allosteric effect.

In practice, K^0_{iy} and Q_{ay} are determined by plotting either $K_{1/2}$ from eq 1 or the reciprocal of $k_{cat}/K_{1/2}$ from eq 2 versus the PEP concentration and fitting these data to the following equation as previously described:[8]

$$K_a = K^0_{ia}\frac{K^0_{iy} + [Y]}{K^0_{iy} + Q_{ay}[Y]} \quad (4)$$

where K_a is equal to $K_{1/2}$ when data were fit to eq 1 or $K_{1/2}/k_{cat}$ when data were fit to eq 2 and [Y] is the concentration of PEP.

RESULTS

As documented by Shirmer and Evans,[3] BsPFK undergoes a quaternary shift of ~7° about the dimer−dimer interface that contains the substrate binding sites upon the binding of the inhibitor phosphoglycolate (PGA). This shift causes a concomitant unwinding of the last turn of helix 6 as shown in Figure 1. The loop that forms when PGA is bound contains residues 156−160. In the Fru-6-P- and MgADP-bound BsPFK crystal structure, D12 interacts with T156, S159, and H160 in the adjacent subunit when it is in the helix configuration (Figure 1A). In the PGA-bound BsPFK structure, D12 interacts with only T158 across the interface and not with the other residues of the loop (Figure 1B). Thus, D12, which is 100% conserved in bacteria containing PFK-1, exhibits a complete change in its interacting partners when the inhibitor binds. T156, also 100% conserved, experiences a change in interacting partners as well, from D12 when Fru-6-P and MgADP are bound to Y164 (an intrasubunit interaction not shown in Figure 1) when the inhibitor is bound.

The specific activities of wild-type and D12A BsPFK are shown Figure 2 as a function of Fru-6-P concentration. Equation 1 was used to fit these data. However, the apparent dissociation constant for Fru-6-P ($K_{1/2}$) from D12A BsPFK is substantially increased compared to that of the wild type, which makes performing complete Fru-6-P titrations in the presence of inhibitor impossible because of the inability to achieve saturation by substrate. Therefore, to measure the nature and magnitude of the allosteric effect between Fru-6-P and PEP for

dx.doi.org/10.1021/bi4002503 | Biochemistry 2013, 52, 5421−5429

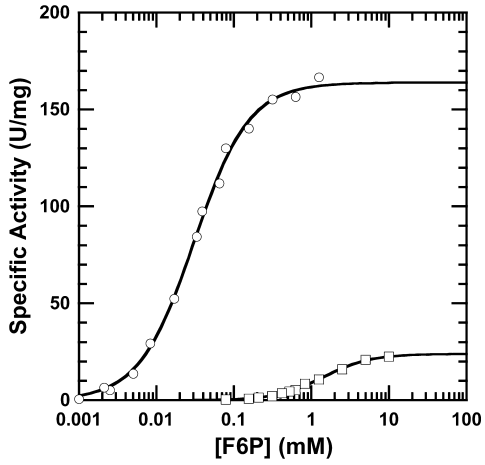

Figure 2. Specific activity vs Fru-6-P concentration for wild-type and D12A BsPFK. Data for wild-type BsPFK are represented by circles, and data for D12A BsPFK are represented by squares. Solid lines represent the best fits of the data to eq 1.

D12A BsPFK and other variants exhibiting low affinity, only data in the linear region of the Fru-6-P titration curves at low Fru-6-P concentrations were examined and fit to eq 2. The slope of this linear region is equal to $k_{cat}/K_{1/2}$ and reflects the first binding of Fru-6-P to the enzyme.

Figure 3 compares plotting $K_{1/2}$ or $K_{1/2}/k_{cat}$ versus PEP concentration for wild-type BsPFK to demonstrate the validity

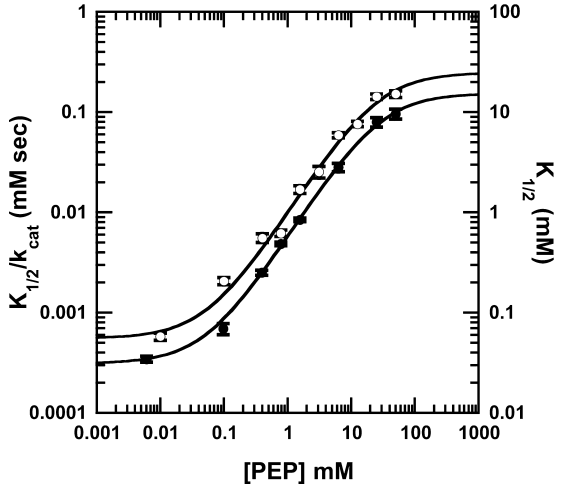

Figure 3. Plots of $K_{1/2}/k_{cat}$ and $K_{1/2}$ vs PEP concentration for wild-type BsPFK. $K_{1/2}/k_{cat}$ values are shown with empty circles and was determined as described in the text. $K_{1/2}$ values are shown with filled circles. Solid lines represent the best fits of each data set to eq 4.

of using $K_{1/2}/k_{cat}$ in eq 3. The apparent dissociation constant for PEP in the absence of Fru-6-P, K^0_{iy}, and the coupling parameter, Q_{ay}, determined from both methods agree within error as can be seen by the similar dependence of the transition on PEP concentration and the similar distance between the plateau values, respectively.[8] The apparent dissociation constant for Fru-6-P, K^0_{ia}, is the only parameter of eq 3 that is not comparable between the two techniques. However, by simply fitting eq 1 to a Fru-6-P titration curve in the absence of PEP, we can approximate K^0_{ia} as being equal to $K_{1/2}$ from this fit. Subsequent $K_{1/2}$ values as a function of PEP concentration can then be calculated for the purpose of comparison by normalizing to this value, assuming that k_{cat} remains relatively constant. This analysis assumes that the rapid equilibrium assumption with respect to Fru-6-P binding remains valid as the PEP concentration is varied as we have found to be the case for wild-type BsPFK.[28]

Figure 4A illustrates the normalized $K_{1/2}$ values versus PEP concentration for D12A BsPFK versus the wild type. Kinetic

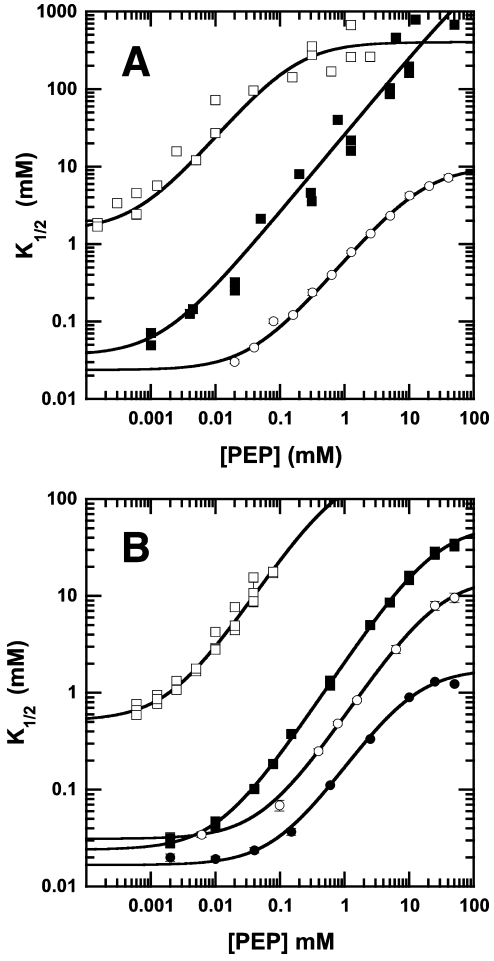

Figure 4. (A) Influence of PEP on the $K_{1/2}$ for the wild type and the apparent $K_{1/2}$ for D12A and H160A variants of BsPFK. Data for the wild type are represented by circles, data for D12A by empty squares, and data for H160A by filled squares. (B) Influence of PEP on the $K_{1/2}$ of the wild type and the apparent $K_{1/2}$ for T156A, T158A, and S159A variants of BsPFK. Data for the wild type are represented by empty circles, data for T156A by empty squares, data for T158A by filled circles, and data for S159A by filled squares. Solid lines represent the best fits to eq 3.

and coupling parameters derived from these data are presented in Table 2. D12A BsPFK exhibits a dissociation constant for Fru-6-P, K^0_{ia}, of 1.4 ± 0.1 mM, which is almost 50-fold greater than the dissociation constant for the substrate from wild-type BsPFK. By contrast, D12A BsPFK has a dissociation constant for PEP, K^0_{iy}, equal to 0.45 ± 0.01 μM, which is ~100-fold smaller than K^0_{iy} for the wild type. Most striking, however, is the fact that despite these large differences in binding affinities, the coupling parameter between Fru-6-P and PEP for D12A is remarkably similar to that of the wild type.

The values of $K_{1/2}$ versus the PEP concentration for the wild type and the other variants of BsPFK are also shown in panels

dx.doi.org/10.1021/bi4002503 | *Biochemistry* 2013, 52, 5421−5429

Table 2. Steady-State Kinetic and Coupling Parameters for Variant BsPFKs

	specific activity (units/mg)	K^0_{ia} (mM)	K^0_{iy} (μM)	Q_{ay}
wild type	163 ± 3	0.030 ± 0.002	60 ± 4	0.0020 ± 0.0003
D12A	24 ± 1	1.4 ± 0.1	0.45 ± 0.01	0.0030 ± 0.0001
H160A	70 ± 2	0.056 ± 0.002	1.0 ± 0.1	<0.00001
T156A	50 ± 3	0.52 ± 0.01	2.1 ± 0.1	0.002 ± 0.001
T158A	70 ± 3	0.017 ± 0.001	98 ± 4	0.009 ± 0.001
S159A	140 ± 4	0.025 ± 0.003	12 ± 1	0.0005 ± 0.0001

A and B of Figure 4, and the kinetic and coupling parameters for these forms are listed in Table 2. The dissociation constants for dissociation of Fru-6-P from T158A, S159A, and H160A are comparable to the dissociation constant of wild-type BsPFK. However, the K^0_{ia} for T156A is 0.52 ± 0.005 mM, which represents a 17-fold decrease in the substrate binding affinity compared to that of the wild type. The PEP binding affinities of the mutant BsPFKs are a bit more varied. T156A, S159A, and H160A all exhibit enhanced PEP binding affinity, though to different degrees. T158A, unlike the other variants, exhibits a diminished PEP binding affinity of almost 2-fold compared to that of the wild type. D12A and T156A BsPFKs are the only two variants that show a significant enhancement of PEP binding affinity while also exhibiting a diminished Fru-6-P binding affinity.

The coupling constants of the variants of BsPFK vary dramatically depending on the mutation. T158A is the only mutant BsPFK that shows a significant decrease in its extent of coupling, as conveyed by an increase in the value of Q_{ay}. Both S159A and H160A BsPFKs exhibit enhanced coupling, when compared to that of the wild type, while the coupling parameters for T156A and D12A BsPFK are remarkably similar to those of wild-type and D12A BsPFKs.

Diffraction-quality crystals of D12A bound to PEP were obtained, and a structural model that was consistent with data obtained by X-ray crystallography was created. The PEP binding of this mutant is enhanced to such a degree that the endogenous PEP stayed bound to the enzyme throughout the extensive purification and dialysis processes. The crystals belong to space group $P2_12_12_1$ with the following unit cell dimensions: a = 96.65 Å, b = 112.97 Å, and c = 131.04 Å. The asymmetric unit consists of one tetramer. The final structure was refined to R factor and R_{free} values of 18.86 and 23.48%, respectively, using diffraction data to 2.0 Å resolution. Given the kinetic and coupling similarities between D12A BsPFK and T156A BsPFK, diffraction-quality crystals of T156A BsPFK were also obtained and a model of the structure was determined. The crystal structure of T156A BsPFK also has four PEP molecules bound to the effector binding sites. The crystals belong to the same space group as crystals of PEP-bound D12A BsPFK and are similar. The final structure was refined to R factor and R_{free} values of 16.6 and 23.78%, respectively, to a resolution of 2.5 Å. The details describing the diffraction data and refinement statistics are listed in Table 1. Coordinates for these structures have been deposited in the Protein Data Bank as entries 4I7E and 4I4I, respectively.

The fact that PEP remained bound to the mutant enzymes after purification from an *E. coli* lysate demonstrates the extremely tight PEP binding of D12A and T156A BsPFKs. The purification process included two columns, one of which is a strong anion exchange column, as well as numerous dialysis steps. The binding antagonism between Fru-6-P and PEP with respect to BsPFK was exploited in removing PEP from D12A BsPFK. Specifically, D12A BsPFK was dialyzed against a solution containing Fru-6-P for more than 48 h, followed by dialysis for at least 24 h against buffer containing no ligand. Diffraction-quality crystals of apo D12A BsPFK were obtained and showed packing similar to that of the PEP-bound crystals. The asymmetric unit consists of a single tetramer. The final structure was refined to R factor and R_{free} values of 20.07 and 25.39%, respectively, to a resolution of 2.3 Å. The details describing the diffraction data and refinement statistics are listed in Table 1, and the coordinates have been deposited in the Protein Data Bank as entry 4I36. Several attempts using the same strategy were made to crystallize an apo form of T156A BsPFK. However, every crystal form contained PEP, which might suggest that apo T156A is unstable.

No large structural differences between the apo and PEP-bound forms of D12A BsPFK and the PEP-bound form of T156A are evident. Figure 5 compares the D12 region of these structures. All three structures exhibit the quaternary shifted position closely resembling that found in the PGA-bound wild-type BsPFK structure as revealed by residues 156−160 forming a loop rather than a helix as shown in Figure 1B. In addition, the active sites are comparable among the three inhibited forms of BsPFK (data not shown).

Figure 6A is an overlay of the residues in the effector binding site for the apo and PEP structures of D12A BsPFK. In the PEP-bound structure of D12A, K214 forms a hydrogen bond with Y69, a hydrogen bond that does not exist in the apo version of D12A. The hydrogen bond formed between K214 and Y69 pulls K214 out of the binding pocket and causes H215 to tilt toward the CH_2 group of PEP. The change in the orientation of D59 observed between the apo and PEP-bound D12A structures is a result of the ligand binding because the same residue overlays perfectly with the PGA-bound structure of the wild type. Figure 6B is an overlay of the effector site residues in the PEP-bound D12A structure and in the PGA-bound wild-type structure. The positions of the residues are very similar between the inhibitor-bound proteins except for K214 and H215. The imidazole ring of H215 is closer to the CH_2 group of PEP in the D12A structure, and in the PGA structure, the ring is oriented away from the ligand.

Comparisons of the B factor distributions for the variant BsPFK crystal structures suggest that the dynamics of these structures are remarkably similar to each other as well (data not shown). Overall, the B factors of the variant structures resemble those of apo wild-type BsPFK.[26]

DISCUSSION

The mechanism proposed by Schirmer and Evans to explain the allosteric behavior of BsPFK attributes the PEP inhibition to the conformational changes observed between the two crystal structures of BsPFK, the Fru-6-P- and MgADP-bound structure and the PGA-bound structure.[3] In contrast, the study presented here, as well as previous studies conducted with BsPFK,[9,10,27,28]

dx.doi.org/10.1021/bi4002503 | *Biochemistry* 2013, 52, 5421−5429

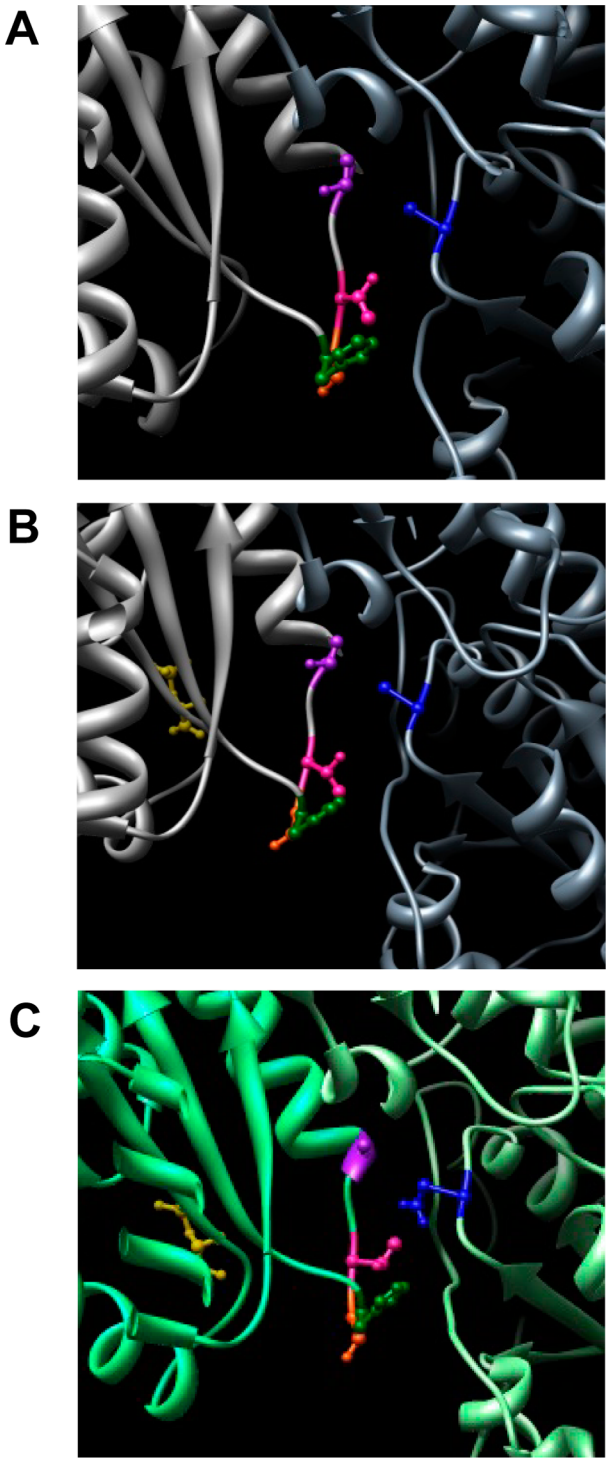

Figure 5. Comparison of the D12 region of D12A and T156A variants of BsPFK: (A) apo D12A, (B) D12A with PEP bound, and (C) T156A with PEP bound. D12A BsPFK is shown as a gray ribbon and T156A BsPFK as a green ribbon. Residue D12 (or D12A) is colored blue, T156 (or T156A) purple, T158 pink, S159 orange, and H160 green. PEP is colored gold.

provides evidence that is difficult to reconcile with this proposal. The crystal structure of apo D12A BsPFK indicates that the enzyme has undergone the quaternary shift previously associated with the binding of the inhibitor; however, analysis of its coupling parameters shows that the mutant enzyme exhibits an extent of inhibition by PEP that is nearly equivalent

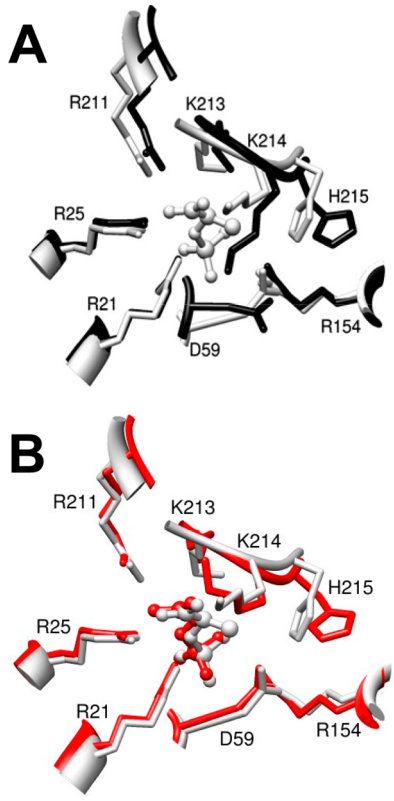

Figure 6. (A) Overlay of residues in the effector binding site of D12A BsPFK. The apo form is colored black and the PEP-bound structure light gray. PEP is shown in ball-and-stick mode. (B) Overlay of residues in the effector binding site for inhibitor-bound BsPFK. Wild-type PGA-bound BsPFK is colored red, with PGA depicted in ball-and-stick mode. PEP-bound D12A is colored gray, with PEP depicted in ball-and-stick mode.

to that of the wild type. If the quaternary shift and the associated conformational changes including the unwinding of the 156−160 helical turn are responsible for PEP inhibition, then D12A BsPFK should not exhibit further inhibition upon the binding of PEP. In essence, one would expect the mutant enzyme to exhibit characteristics similar to those of the wild-type enzyme that had already been saturated by inhibitor. Indeed, D12A BsPFK exhibits a Fru-6-P binding in the absence of PEP that is comparable to the Fru-6-P binding of the wild type when PEP is saturating. However, even with the poor Fru-6-P binding that D12A BsPFK exhibits, the mutant enzyme still shows further heterotropic inhibition by PEP of a magnitude that is comparable to that of the wild type.

Given that D12 potentially interacts with multiple residues across the substrate interface, the role of each potential interaction was assessed through mutagenesis, followed by kinetic and coupling analysis. T158 is the only residue across the substrate interface from D12 that seems to interact with D12 when the inhibitor is bound to the enzyme, and it is the only potential D12 interaction that is not highly conserved. T158A is also the only mutant enzyme tested that showed a significant enhancement of Fru-6-P binding affinity and a diminished PEP binding affinity. In addition, T158A is the only mutation that showed a diminished coupling parameter. These data suggest that the potential hydrogen bond formed between D12 and T158 when PEP is bound to the enzyme is not responsible for the D12A BsPFK binding and coupling characteristics.

dx.doi.org/10.1021/bi4002503 | *Biochemistry* 2013, 52, 5421−5429

Likewise, the binding characteristics of S159A BsPFK and H160A BsPFK do not follow the trends seen with D12A BsPFK. While S159A does cause a slight enhancement in PEP binding affinity, the Fru-6-P binding remains comparable to that of the wild type. H160A does enhance PEP affinity to nearly the same level as does D12A, but the Fru-6-P affinity is within a factor of 2 of that of the wild type. Interestingly, the coupling coefficients for S159A BsPFK and H160A BsPFK show much greater inhibition than that of the wild type. In fact, the coupling of H160A BsPFK cannot be accurately estimated because fully saturating amounts of Fru-6-P and PEP cannot be produced. Unfortunately, all crystals grown for H160A BsPFK so far have diffracted to only low resolution.

By contrast, both T156 and D12 are located along the substrate-binding interface, directly across from each other when Fru-6-P and MgADP are bound. Both residues are 100% conserved among all available bacterial type 1 ATP-dependent PFK sequences. Neither residue directly interacts with a ligand. In addition, when each residue is replaced with an alanine, the coupling and kinetic characteristics are also similar to each other. D12A and T156A enhance PEP binding 100- and 28-fold, respectively, and weaken Fru-6-P binding 50- and 17-fold, respectively. However, the coupling parameters exhibited by D12A and T156A are each remarkably similar to that of the wild type.

While it is possible to rationalize why the disruption of the D12−T156 interaction could destabilize the subunit interface sufficiently to allow the quaternary shift to occur, it is more difficult to understand why this significant conformational perturbation seems not to influence the allosteric coupling between Fru-6-P and PEP. One possibility is that the structures do not paint the whole picture. K-Type allostery, by its very nature, is a thermodynamic phenomenon that is composed of both enthalpic and entropic components. Static structural models obtained by whatever means, though informative, do not directly address dynamics and should be considered to reveal but one aspect of a thermodynamic allosteric mechanism. Another possibility is that the allosteric communication occurs primarily between sites within individual subunits. Monomeric and single-domain proteins have been shown to be allosteric.[29−31] Quaternary structural changes need not be a requirement for allostery.

The diminished maximal specific activity of D12A BsPFK when compared to that of wild-type BsPFK is a potential complication to the interpretation of the functionality of this variant. It seems likely, however, that the lower k_{cat} is related to the interaction of D12 with R252 rather than its interactions with residues 156−160. R252 forms intrasubunit interactions with both D12 and Fru-6-P when it is bound. Previous comparisons of mutant enzymes R252A and R252A/D12A to each other and the wild type reveal that the introduction of the D12A mutation into the R252A variant did not substantially alter the maximal specific activity of the enzyme.[10,13] The D12A enzyme forms stable homotetramers, in the presence and absence of PEP. A comparison of the active sites of apo D12A and apo wild-type BsPFKs shows a very small perturbation in the orientation of R252 when it interacts with Fru-6-P in the wild-type enzyme. The D12−R252 interaction, when completely removed in the double mutant, may allow for the proper orientation of the substrate in the binding pocket. However, if the negative charge of D12 is removed and the positive charge of R252 is thereby unrestrained, then an altered orientation of R252 may interfere with the binding of Fru-6-P in the proper orientation. To address this possibility, we have unsuccessly attempted to produce crystals of D12A BsPFK bound to Fru-6-P.

Schirmer and Evans assumed that the PGA BsPFK structure is equivalent to the PEP-bound structure. Indeed, the structures of the PEP-bound variants of BsPFK and PGA-bound wild-type BsPFK would suggest that this assumption was appropriate because the structures are very similar. In particular, the structures of the effector binding pockets of PGA-bound wild-type BsPFK, apo D12A BsPFK, and PEP-bound D12A BsPFK are quite analogous. It is also true, however, there are no obvious structural explanations within the binding site for why PEP binds to D12A BsPFK 100-fold tighter than PGA (and PEP) does to the wild type.

Given these observations, we feel it is possible that the quaternary shift, envisioned at one time as a key component to the mechanism for allosteric inhibition of BsPFK, may instead have an influence on ligand binding that is remote from the binding sites but does not influence allosteric inhibition per se. D12A BsPFK and likely T156A BsPFK, which have undergone the quaternary shift, exhibit significant changes in ligand binding compared to that of the wild type, yet they possess allosteric coupling constants that are comparable to that of the wild type. Further investigations into how the inhibition influences the structure and dynamics of BsPFK must be conducted before a comprehensive mechanism for allosteric inhibition can be proposed.

Possibly more to the point, from the definition given in eq 3, it can easily be shown that the coupling parameter, Q_{ay}, represents the equilibrium constant for the following disproportionation equilibrium:

$$\text{Y-E} + \text{E-A} \overset{Q_{ay}}{\longleftrightarrow} \text{Y-E-A} + \text{E} \quad (5)$$

where Y-E represents the inhibitor-bound enzyme, E-A represents the substrate-bound enzyme, E represents the free enzyme, and Y-E-A represents the ternary complex of the enzyme with both inhibitor and substrate bound. The structures considered by Schirmer and Evans, and indeed the structures presented in this report, all relate to the enzyme forms depicted on the left-hand side of this equilibrium. However, the question of why PEP inhibits PFK must be answered by understanding why this equilibrium is poised in favor of those left-hand-side components. This answer cannot be formulated without an understanding of the features associated with those components on the right-hand side. We have recently published the structure of apo BsPFK, i.e., E, that provides an important component of this information.[26] However, it is structural information (including dynamics) regarding the ternary complex, Y-E-A, that will provide ultimately the key to unlocking the answer to the question of why PEP inhibits the binding of Fru-6-P. Unfortunately, so far, structural information pertaining to the ternary complex has remained elusive.

AUTHOR INFORMATION

Corresponding Author

*Department of Biochemistry and Biophysics, Texas A&M University, 2128 TAMU, College Station, TX 77843-2128. E-mail: gdr@tamu.edu. Phone: (979) 862-2263.

Present Addresses

†R.M.: Department of Molecular Physiology and Biophysics, Vanderbilt University Medical Center, Nashville, TN 37232.

‡J.B.B.: School of Molecular and Biomedical Science, University of Adelaide, Adelaide, Australia.

Funding

This work was supported by National Institutes of Health Grant GM033216 and Robert A. Welch Foundation Grant A1543 to G.D.R.

Notes

The authors declare no competing financial interest.

■ ABBREVIATIONS

PFK, phosphofructokinase; Fru-6-P, fructose 6-phosphate; F1,6BP, fructose 1,6-bisphosphate; BsPFK, phosphofructokinase from *B. stearothermophilus*; PEP, phosphoenolpyruvate; PGA, phosphoglycolate; MOPS, 3-(*N*-morpholino)-propanesulfonic acid; DTT, dithiothreitol; EPPS, *N*-(2-hydroxyethyl)piperazine-*N*′-(3-propanesulfonic acid); SDS–PAGE, sodium dodecyl sulfate–polyacrylamide gel electrophoresis.

■ REFERENCES

(1) Blangy, D., Buc, H., and Monod, J. (1968) Kinetics of the allosteric interactions of phosphofructokinase from *Escherichia coli*. *J. Mol. Biol. 31*, 13–35.

(2) Monod, J., Wyman, J., and Changeux, J. P. (1965) On the nature of allosteric transitions: A plausible model. *J. Mol. Biol. 12*, 88–118.

(3) Schirmer, T., and Evans, P. R. (1990) Structural basis of the allosteric behaviour of phosphofructokinase. *Nature 343*, 140–145.

(4) Evans, P. R., and Hudson, P. J. (1979) Structure and control of phosphofructokinase from *Bacillus stearothermophilus*. *Nature 279*, 500–504.

(5) Evans, P. R., Farrants, G. W., and Hudson, P. J. (1981) Phosphofructokinase: Structure and control. *Philos. Trans. R. Soc., B 293*, 53–62.

(6) Krauss, G. (2001) *Biochemistry of signal transduction and regulation*, 2nd ed., Wiley-VCH, Weinheim, Germany.

(7) Voet, D., Voet, J. G., and Pratt, C. W. (2008) *Fundamentals of biochemistry: Life at the molecular level*, 3rd ed., John Wiley & Sons, Hoboken, NJ.

(8) Reinhart, G. D. (2004) Quantitative analysis and interpretation of allosteric behavior. *Methods Enzymol. 380*, 187–203.

(9) Kimmel, J. L., and Reinhart, G. D. (2000) Reevaluation of the accepted allosteric mechanism of phosphofructokinase from *Bacillus stearothermophilus*. *Proc. Natl. Acad. Sci. U.S.A. 97*, 3844–3849.

(10) Ortigosa, A. D., Kimmel, J. L., and Reinhart, G. D. (2004) Disentangling the web of allosteric communication in a homotetramer: Heterotropic inhibition of phosphofructokinase from *Bacillus stearothermophilus*. *Biochemistry 43*, 577–586.

(11) French, B. A., Valdez, B. C., Younathan, E. S., and Chang, S. H. (1987) High-level expression of *Bacillus stearothermophilus* 6-phosphofructo-1-kinase in *Escherichia coli*. *Gene 59*, 279–283.

(12) Lovingshimer, M. R., Siegele, D., and Reinhart, G. D. (2006) Construction of an inducible, *pfkA* and *pfkB* deficient strain of *Escherichia coli* for the expression and purification of phosphofructokinase from bacterial sources. *Protein Expression Purif. 46*, 475–482.

(13) Valdez, B. C., French, B. A., Younathan, E. S., and Chang, S. H. (1989) Site-directed mutagenesis in *Bacillus stearothermophilus* fructose-6-phosphate 1-kinase. Mutation at the substrate-binding site affects allosteric behavior. *J. Biol. Chem. 264*, 131–135.

(14) Riley-Lovingshimer, M. R., and Reinhart, G. D. (2001) Equilibrium binding studies of a tryptophan-shifted mutant of phosphofructokinase from *Bacillus stearothermophilus*. *Biochemistry 40*, 3002–3008.

(15) Otwinowski, Z., Minor, W., and Carter, C. W., Jr. (1997) Processing of X-ray diffraction data collected in oscillation mode. *Methods Enzymol. 276*, 307–326.

(16) Pflugrath, J. W. (1999) The finer things in X-ray diffraction data collection. *Acta Crystallogr. D55*, 1718–1725.

(17) McCoy, A. J. (2007) Solving structures of protein complexes by molecular replacement with Phaser. *Acta Crystallogr. D63*, 32–41.

(18) Adams, P. D., Grosse-Kunstleve, R. W., Hung, L. W., Ioerger, T. R., McCoy, A. J., Moriarty, N. W., Read, R. J., Sacchettini, J. C., Sauter, N. K., and Terwilliger, T. C. (2002) PHENIX: Building new software for automated crystallographic structure determination. *Acta Crystallogr. D58*, 1948–1954.

(19) Selvanayagam, S., Welmurugan, D., and Yamane, T. (2006) Iterative ACORN as a high throughput tool in structural genomics. *Indian J. Biochem. Biophys. 43*, 211–216.

(20) Winn, M. D., Isupov, M. N., and Murshudov, G. N. (2001) Use of TLS parameters to model anisotropic displacements in macromolecular refinement. *Acta Crystallogr. D57*, 122–133.

(21) Emsley, P., and Cowtan, K. (2004) Coot: Model-building tools for molecular graphics. *Acta Crystallogr. D60*, 2126–2132.

(22) Davis, I. W., Leaver-Fay, A., Chen, V. B., Block, J. N., Kapral, G. J., Wang, X., Murray, L. W., Arendall, W. B., III, Snoeyink, J., Richardson, J. S., and Richardson, D. C. (2007) MolProbity: All-atom contacts and structure validation for proteins and nucleic acids. *Nucleic Acids Res. 35*, W375–W383.

(23) Hill, A. V. (1910) A new mathematical treatment of changes of ionic concentration in muscle and nerve under the action of electric currents, with a theory as to their mode of excitation. *J. Physiol. 40*, 190–224.

(24) Reinhart, G. D. (1983) The determination of thermodynamic allosteric paramters of an enzyme undergoing steady-state turnover. *Arch. Biochem. Biophys. 224*, 389–401.

(25) Reinhart, G. D. (1988) Linked-function origins of cooperativity in a symmetrical dimer. *Biophys. Chem. 30*, 159–172.

(26) Mosser, R., Reddy, M. C., Bruning, J. B., Sacchettini, J. C., and Reinhart, G. D. (2012) Structure of the apo form of *Bacillus stearothermophilus* phosphofructokinase. *Biochemistry 51*, 769–775.

(27) Braxton, B. L., Tlapak-Simmons, V. L., and Reinhart, G. D. (1994) Temperature-induced inversion of allosteric phenomena. *J. Biol. Chem. 269*, 47–50.

(28) Tlapak-Simmons, V. L., and Reinhart, G. D. (1994) Comparison of the inhibition by phospho(*enol*)pyruvate and phosphoglycolate of phosphofructokinase from *B. stearothermophilus*. *Arch. Biochem. Biophys. 308*, 226–230.

(29) Gunasekaran, K., Ma, B., and Nussinov, R. (2004) Is allostery an intrinsic property of all dynamic proteins? *Proteins: Struct., Funct., Bioinf. 57*, 433–443.

(30) Swain, J. F., and Gierasch, L. M. (2006) The changing landscape of protein allostery. *Curr. Opin. Struct. Biol. 16*, 102–108.

(31) Kolb, D. A., and Weber, G. (1975) Cooperativity of binding of anilinonaphthalenesulfonate to serum albumin induced by a second ligand. *Biochemistry 14*, 4476–4481.